



Beyond Autoantibodies: Biologic Roles of Human Autoreactive B Cells in Rheumatoid Arthritis Revealed by RNA-Sequencing

Ankit Mahendra,¹ Xingyu Yang,² Shaza Abnoui,¹ Jay R. T. Adolacion,¹ Daechan Park,³ Sanam Soomro,¹ Jason Roszik,⁴ Cristian Coarfa,⁵ Gabrielle Romain,¹ Keith Wanzeck,⁶ S. Louis Bridges Jr.,⁶  Amita Aggarwal,⁷ Peng Qiu,² Sandeep K. Agarwal,⁵ Chandra Mohan,¹ and Navin Varadarajan¹ 

Objective. To obtain the comprehensive transcriptome profile of human citrulline-specific B cells from patients with rheumatoid arthritis (RA).

Methods. Citrulline- and hemagglutinin-specific B cells were sorted by flow cytometry using peptide–streptavidin conjugates from the peripheral blood of RA patients and healthy individuals. The transcriptome profile of the sorted cells was obtained by RNA-sequencing, and expression of key protein molecules was evaluated by aptamer-based SOMAscan assay and flow cytometry. The ability of these proteins to effect differentiation of osteoclasts and proliferation and migration of synoviocytes was examined by in vitro functional assays.

Results. Citrulline-specific B cells, in comparison to citrulline-negative B cells, from patients with RA differentially expressed the interleukin-15 receptor α (IL-15R α) gene as well as genes related to protein citrullination and cyclic AMP signaling. In analyses of an independent cohort of cyclic citrullinated peptide–seropositive RA patients, the expression of IL-15R α protein was enriched in citrulline-specific B cells from the patients' peripheral blood, and surprisingly, all B cells from RA patients were capable of producing the epidermal growth factor ligand amphiregulin (AREG). Production of AREG directly led to increased migration and proliferation of fibroblast-like synoviocytes, and, in combination with anti–citrullinated protein antibodies, led to the increased differentiation of osteoclasts.

Conclusion. To the best of our knowledge, this is the first study to document the whole transcriptome profile of autoreactive B cells in any autoimmune disease. These data identify several genes and pathways that may be targeted by repurposing several US Food and Drug Administration–approved drugs, and could serve as the foundation for the comparative assessment of B cell profiles in other autoimmune diseases.

INTRODUCTION

The identification of citrullination has been a major milestone in the study of rheumatoid arthritis (RA) (1,2). Citrullination is the posttranslational modification of arginine residues to citrulline in proteins, catalyzed by peptidyl arginine deiminase (PAD) enzymes, as one of the key factors mediating the breach in tolerance and eliciting anti–citrullinated protein antibody (ACPA) responses. The appearance of ACPAs in the circulation precedes the onset of clin-

ical disease, and ACPA positivity has a sensitivity of 60–70%, and a specificity of >90%, for the diagnosis of RA (1). ACPAs have been shown to trigger human immune effector functions, including activation of the complement system and the ability to engage activating Fc γ receptors (3). In addition, it has been demonstrated that ACPAs can catalyze the bone erosion commonly seen in RA patients (4).

Although the indispensable role of B cells in autoantibody production is well recognized, their autoantibody-independent

Supported by the Cancer Prevention and Research Institute of Texas (RP130570 and RP180466), the United States Department of Defense (Congressional Directed Medical Research Program CA160591), the Melanoma Research Alliance (509800), the National Science Foundation (1705464), the NIH (grant R01-CA-174385), the Owens Foundation, the Welch Foundation (E-1774), and the University of Alabama at Birmingham RADAR fund.

¹Ankit Mahendra, PhD, Shaza Abnoui, BS, Jay R. T. Adolacion, MS, Sanam Soomro, BS, Gabrielle Romain, PhD, Chandra Mohan, MD, PhD, Navin Varadarajan, PhD: University of Houston, Houston, Texas; ²Xingyu Yang, BS, Peng Qiu, PhD: Georgia Institute of Technology, Atlanta; ³Daechan Park, PhD: Ajou University, Suwon, Republic of Korea; ⁴Jason Roszik, PhD: University

of Texas MD Anderson Cancer Center, Houston; ⁵Cristian Coarfa, PhD, Sandeep K. Agarwal, MD, PhD: Baylor College of Medicine, Houston, Texas; ⁶Keith Wanzeck, MS, S. Louis Bridges Jr., MD, PhD: University of Alabama at Birmingham; ⁷Amita Aggarwal, MD: Sanjay Gandhi Postgraduate Institute of Medical Sciences, Lucknow, India.

No potential conflicts of interest relevant to this article were reported.

Address correspondence to Navin Varadarajan, PhD, Department of Chemical & Biomolecular Engineering, University of Houston, 4726 Calhoun Road, Houston, Texas 77204-4005. E-mail: nvaradar@central.uh.edu.

Submitted for publication May 10, 2018; accepted in revised form November 1, 2018.

contributions are not as well-defined. Systemic depletion of B cells using rituximab, a strategy that targets B cells expressing human CD20 (a phenotypic cell surface marker), has been shown to be effective clinically for the treatment of a subset of RA patients (5). Although studies have supported the idea that patients with higher autoantibody titers are likely to respond to rituximab (6), the clinical efficacy of rituximab treatment is not necessarily correlated with a decrease in autoantibody titers (7). This, in turn, implies a more expanded role for B cells in autoimmune pathogenicity beyond antibody production.

Preclinical and clinical data have suggested many different functions of B cells in RA, including 1) a role as antigen-presenting cells (8), 2) direct secretion of proinflammatory cytokines, such as tumor necrosis factor (TNF) and interleukin-6 (IL-6) (9–11), that support the organization of tertiary lymphoid tissues within the inflamed synovium (8,12), and 3) an effect on bone homeostasis through the secretion of RANKL (13). Despite these efforts, a direct interrogation of the roles of the autoreactive B cell compartment, and how they differ from other B cells from the same donor or from B cells from healthy individuals, has not been accomplished.

One of the major challenges in profiling autoreactive B cells within humans is the low frequency of these cells in peripheral blood (<0.1% of all B cells in the circulation) (14). We developed and validated a flow cytometry-based assay for the reliable detection of cyclic citrullinated peptide (CCP)-specific B cells *ex vivo*. We then performed RNA-sequencing (RNA-seq) on these small numbers of cells with the purpose of comparing the whole transcriptome profile of RA-CCP-specific (RA-CCP^{POS}) B cells to that of RA-CCP-negative (RA-CCP^{NEG}) B cells from the same donor and to that of hemagglutinin-specific (HA^{POS}) B cells from healthy individuals elicited upon vaccination with seasonal influenza virus. We performed a 2-pronged comparison to identify the expression of key genes on all B cells from RA patients that were presumably induced by the systemic proinflammatory environment prevailing in these patients, as well as those genes that were restricted to only autoreactive B cells.

Our data identified a novel role of B cells as an activator of the epidermal growth factor (EGF) pathways by secretion of the EGF receptor ligand amphiregulin (AREG) under proinflammatory conditions, and also identified IL-15 receptor α (IL-15R α) as a specific biomarker of RA-CCP^{POS} B cells. Overall, our data suggest that besides being a source of autoantibodies, B cells may also play direct roles in the inflammatory cascades and osteoclastogenesis in RA. Significantly, while some of the identified genes and pathways are the targets of approved therapies for RA, our data also illustrate that drugs approved for other indications might be useful in targeting the RA-CCP^{POS} B cell compartment in RA. More broadly, to the best of our knowledge, this is the first comprehensive study on the transcriptome profile of human RA-CCP^{POS} B cells in any autoimmune disease, and these data could serve as a resource to further investigate the role of B cells in autoimmunity.

MATERIALS AND METHODS

Patients. Blood samples were obtained from patients with seropositive RA who provided informed consent for study participation under Institutional Review Board–approved protocols at the Baylor College of Medicine, University of Alabama at Birmingham, and University of Houston. Each blood sample (15 ml) was aspirated into heparin vacutainer tubes (BD Biosciences). Details on the patients' demographic and clinical characteristics are summarized in Supplementary Table 1 (available on the *Arthritis & Rheumatology* web site at <http://onlinelibrary.wiley.com/doi/10.1002/art.40772/abstract>). All RA patients met the American College of Rheumatology 1987 classification criteria for RA (15), and all were confirmed to be CCP-seropositive.

Flow cytometric sorting of CCP-specific B cells from RA patients' blood.

Peripheral blood mononuclear cells (PBMCs), isolated from the blood of RA patients by density centrifugation, were blocked with phosphate buffered saline (PBS)–5% human serum for 20 minutes at 4°C. All subsequent staining steps were performed in PBS containing 2% serum. PBMCs were stained for B cell markers with fluorochrome-labeled antibodies, anti-CD19, IgM, and IgD together with a T cell marker using an anti-CD3 antibody (BioLegend) according to the manufacturer's instructions. Biotinylated CCP-I (Anaspec), a surrogate peptide to capture ACPAs, was then added (1 μ g/million PBMCs), followed by labeling with fluorochrome-labeled streptavidin (1 μ g/ml). Subsequently, biotinylated cyclic arginine peptide (CAP; Anaspec) was also added (1 μ g/million PBMCs) as a control, and then labeled with fluorochrome-labeled streptavidin (1 μ g/ml), to exclude B cells cross-reactive to both antigens. Furthermore, CD19^{POS}IgM/IgD^{NEG} B cells (IgG/IgA^{POS}) were gated, and the cell populations CCP^{POS}CAP^{NEG} and CCP^{NEG}CAP^{NEG} were sorted for validation of cell purity.

A total of 125–360 RA-CCP^{POS} B cells were obtained from 10–15 million PBMCs from each patient. The sorted cells were then grown in 96-well tissue culture plates with 1×10^5 /well of 3T3 fibroblast cells secreting msCD40L (NIH AIDS reagent program), 100 ng/ml of IL-21 (PeproTech), and 5 μ g/ml of anti-APO-1 antibody (eBiosciences) for a period of 14 days, with half of the medium changed once after 7 days. Thereafter, cell purity was assessed by validating the specificity of IgG from the culture supernatants against CCP.

Preparation of the complementary DNA (cDNA) library and RNA-sequencing analyses. Total RNA was obtained by sorting antigen-specific B cells (350–1,000 total cells) *ex vivo* directly into 100 μ l of cell lysis buffer, provided in the RNA-XS RNA isolation kit (Macherey-Nagel). Furthermore, cDNA libraries were synthesized using the commercially available

SMART-Seq Ultra Low Input RNA kit (Clontech), in accordance with the manufacturer's protocols. After preparation of cDNA libraries, they were first tagged and then barcoded by indexing primers using the Nexera XT kit (Illumina). The libraries were pooled and a 76-bp paired-end sequencing was performed on an Illumina HiSeq3000 sequencer, to yield a minimum of 17.4 million reads per library (range 17.4–37.3 million).

Details on the methods used for RNA-seq bioinformatics analyses (Gene Expression Omnibus RNA-seq data accession no. GSE99006), purification of ACPAs, fibroblast-like synovio-cyte (FLS) assays, osteoclastogenesis assays, and SOMAmer assays are described in the Supplementary Materials and Methods (available on the *Arthritis & Rheumatology* web site at <http://onlinelibrary.wiley.com/doi/10.1002/art.40772/abstract>).

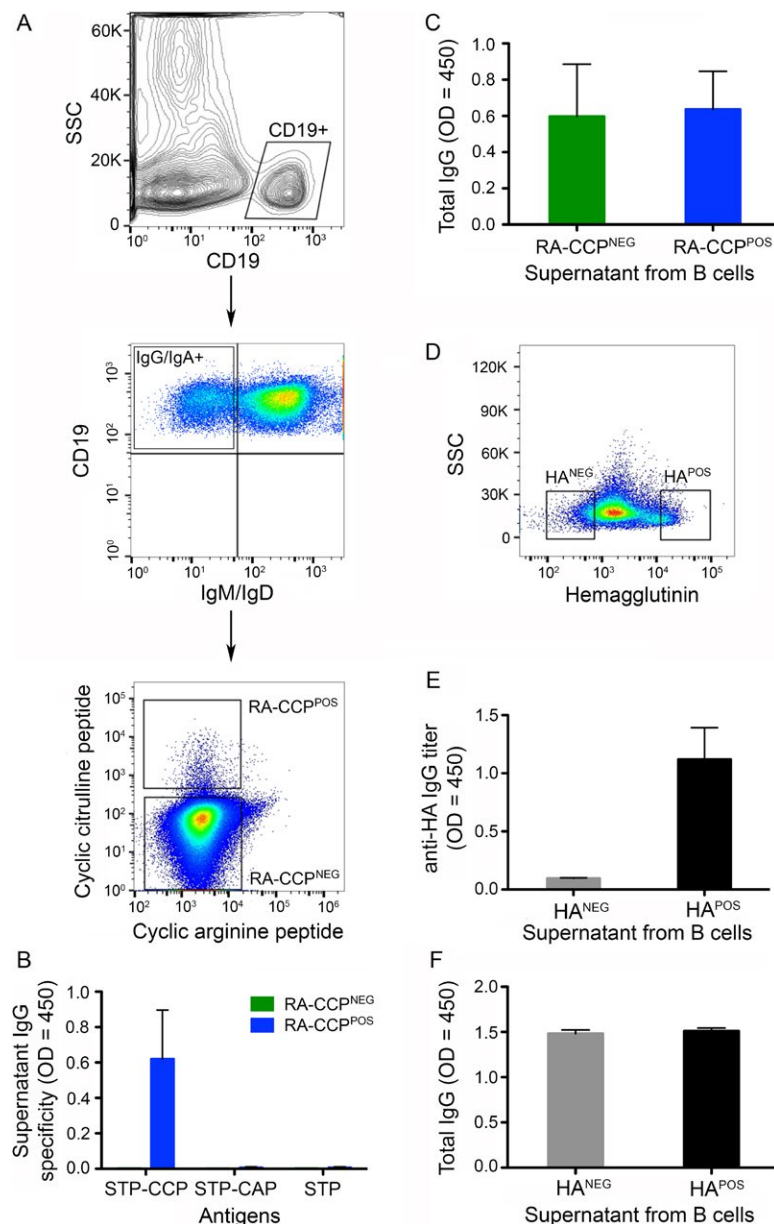


Figure 1. Isolation of an enriched population of rheumatoid arthritis cyclic citrullinated peptide-specific (RA-CCP^{POS}) and hemagglutinin-specific (HA^{POS}) B cells. **A**, Representative flow plots depict the sorting strategy for RA-CCP^{POS} and RA-CCP^{NEG} B cells. Cells were first gated as CD19^{POS}IgM/IgD^{NEG} B cells (IgG/IgA^{POS}); thereafter, RA-CCP^{POS} B cells were sorted by flow cytometry as CCP^{POS}CAP^{NEG} B cells, and RA-CCP^{NEG} cells were sorted as CCP^{NEG}CAP^{NEG} B cells. **B** and **C**, Supernatants (n = 3) were tested by enzyme-linked immunosorbent assay (ELISA) for antigen specificity of RA-CCP^{POS} and RA-CCP^{NEG} B cells (**B**) and for total Ig from RA-CCP^{POS} and RA-CCP^{NEG} B cells (**C**), expanded and differentiated in vitro. **D**, Representative flow plot shows isolation of HA^{POS} and HA^{NEG} B cells, sorted with a similar gating strategy as that described in **A**. **E** and **F**, Supernatants (n = 4) were tested by ELISA for HA reactivity (**E**) and total Ig from HA^{NEG} and HA^{POS} B cell populations (**F**). ELISA results are shown as the mean \pm SEM. STP = streptavidin; CAP = cyclic arginine peptide. Color figure can be viewed in the online issue, which is available at <http://onlinelibrary.wiley.com/doi/10.1002/art.40772/abstract>.

RESULTS

Flow cytometric sorting of antigen-specific B cells.

We developed a dual-labeling flow cytometry method of cell sorting using both CCPs and CAPs to isolate RA-CCP^{POS} B cells. In order to verify the purity of our sorting method, an equal number of B cells within the CCP^{POS}CAP^{NEG} population (hereafter referred to as RA-CCP^{POS} B cells) and CCP^{NEG}CAP^{POS} and CCP^{NEG}-CAP^{NEG} populations (hereafter referred to as RA-CCP^{NEG} B cells) (Figure 1A) were sorted in 96-well plates and grown in vitro for 14 days. The purity of our sorting strategy was validated by testing the supernatants after in vitro culture, which confirmed that only the immunoglobulins secreted in B cell cultures established from the RA-CCP^{POS} B cell population demonstrated a specific reactivity toward the CCP, but not toward streptavidin or the control CAP peptide (Figures 1B and C).

After validation of our sorting strategy, a total of 350–1,000 RA-CCP^{POS} B cells (0.01–0.1%) from the peripheral blood of 4 RA patients were used directly for the preparation of cDNA libraries ex vivo, to ensure minimal perturbations to the transcriptional profile. Both RA-CCP^{POS} and RA-CCP^{NEG} B cells were confirmed to be predominantly of the memory phenotype, based on the surface expression of CD27 and IgD (see Supplementary Figure 1A, <http://onlinelibrary.wiley.com/doi/10.1002/art.40772/abstract>).

For a comparative analysis of the B cell transcriptome profile during autoimmunity compared to that during the normal immune response to vaccination, HA-specific B cells (hereafter referred to as HA^{POS} B cells) were isolated from the peripheral blood of 4 healthy individuals who were vaccinated with the seasonal influenza vaccine. Our ability to enrich for HA^{POS} B cells was validated by the same 3-step procedure as that used for RA-CCP^{POS} B cells: 1) antigen labeling and flow cytometric sorting of a total of 3,500 HA^{POS} and HA^{NEG} cells from PBMCs of these vaccinated donors; 2) in vitro expansion and differentiation; and 3) enzyme-linked immunosorbent assay (ELISA) testing for HA reactivity on the culture supernatants (Figures 1D–F). Similar to the B cells from RA patients, HA^{POS} B cells from healthy individuals also displayed a CD27+ memory phenotype. We did not observe a significant difference in the frequency of memory B cells between different samples of RA-CCP^{POS}, RA-CCP^{NEG}, and HA^{POS} B cells (see Supplementary Figures 1B and C, <http://onlinelibrary.wiley.com/doi/10.1002/art.40772/abstract>).

Subsequent to validation, 1,000–2,000 HA^{POS} B cells from the same 4 healthy donors were used to construct cDNA libraries ex vivo for RNA-seq analyses. In order to ensure that the differences in the gene expression profile of RA-CCP^{POS} B cells was not attributable to the composition of different isotypes of B cells (IgG versus IgA), we analyzed our RNA-seq data for transcripts associated with IgG and IgA molecules, and confirmed that no significant differences were observed between RA-CCP^{POS}, RA-CCP^{NEG}, and HA^{POS} B cells (see Supplementary Figure 1D, <http://onlinelibrary.wiley.com/doi/10.1002/art.40772/abstract>).

Distinguishing RA-CCP^{POS}, RA-CCP^{NEG}, and HA^{POS} B cells based on differentially expressed genes (DEGs).

The cDNA libraries generated ex vivo from the 12 blood samples (comprising 4 paired RA-CCP^{POS} and RA-CCP^{NEG} B cell populations, and 4 HA^{POS} B cell populations) were bar-coded, pooled, and sequenced using 76-bp paired-ends, to yield a minimum of 17 million reads per library. After validation of the RNA-seq populations (see Supplementary Figure 2, <http://onlinelibrary.wiley.com/doi/10.1002/art.40772/abstract>), differential analyses using the DEseq package revealed that 1,658 genes (false discovery rate [FDR] <0.1) were differentially expressed in RA-CCP^{POS} B cells compared to HA^{POS} B cells, and 431 genes were identified as DEGs in RA-CCP^{POS} B cells compared to RA-CCP^{NEG} B cells (see the complete lists provided in Supplementary Tables 3 and 4, <http://onlinelibrary.wiley.com/doi/10.1002/art.40772/abstract>).

We utilized t-distributed stochastic neighbor embedding (t-SNE) to demonstrate that these identified DEGs could clearly resolve the 3 distinct cellular populations (Figure 2A). As expected, both the number of identified DEGs and their relative change in expression were lower in RA-CCP^{POS} B cells compared to RA-CCP^{NEG} B cells from the same donors, in contrast to comparisons between RA-CCP^{POS} B cells and HA^{POS} B cells (see Supplementary Tables 3 and 4). We evaluated the statistical power of our study to differentiate the RA-CCP^{POS} and RA-CCP^{NEG} B cell subsets. Using powsimR (17), we estimated the statistical power of our study to be 0.86 ± 0.18 (mean ± SEM based on 100 simulations).

Comparisons between RA-CCP^{POS} and HA^{POS} B cells.

A number of candidate DEGs whose presence has been well validated in studies of autoimmunity, including the cyclin kinase p21 (*CDKN1A*) (18), ubiquitin ligase *Pell1* (19), and costimulatory molecule *ICOSLG* (20) genes, were identified. The EGF ligand gene *AREG* was identified as the transcript with the largest change in expression (Figure 2B).

By classifying these same DEGs into Gene Ontology categories, we grouped them as being related to B cell activation, genes related to inflammation, and transcription factors. We observed differences in the expression of genes related to B cell activation (Figure 2C), with increased expression of kinase genes such as *PI3KCA* (21) and *MAPK7/MAPK8*, which are known to cause autoimmunity under dysregulated activation (22). In addition, several genes related to inflammation, including signaling molecules such as *TNFAIP3* and *IL6ST* and T cell-recruiting chemokine-like *CCL5* and the chemokine receptor gene *CXCR4* (23,24), were up-regulated in RA-CCP^{POS} B cells (Figure 2D).

Analysis of the differentially expressed transcription factors revealed up-regulation of *PRDM1* and *ETV3* and *ETV3L* within RA-CCP^{POS} B cells; these transcription factors are known to inhibit c-Myc and, consequently, hinder cell growth (25), while at the same time

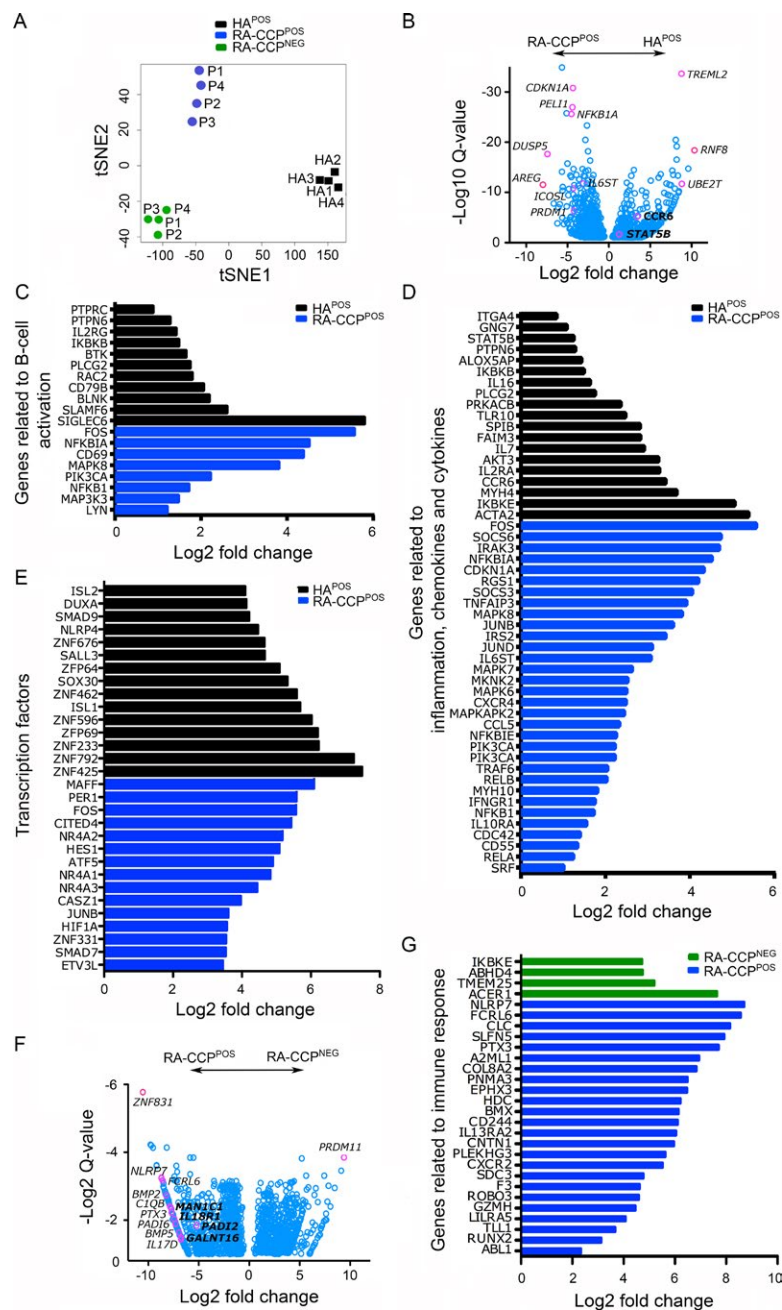


Figure 2. RA-CCP^{POS}, RA-CCP^{NEG}, and HA^{POS} B cells can be differentiated based on differentially expressed genes (DEGs). **A**, For visualization of sample relationships based on differential gene expression, t-distributed stochastic neighbor embedding (t-SNE) was used. P1–4 and HA1–4 represent distinct populations of RA-CCP^{POS} and RA-CCP^{NEG} B cells and HA^{POS} B cells, respectively, based on DEGs. **B**, Volcano plots (generated using the fold change and *q* values of DEGs) show enrichment of genes related to autoimmunity and inflammation in RA-CCP^{POS} B cells compared to HA^{POS} B cells. **C–E**, Gene ontology (GO) plots indicate the fold change in expression of genes related to B cell activation, inflammation, chemokines and cytokines, and the top 15 transcription factors that were differentially enriched in RA-CCP^{POS} compared to HA^{POS} B cells. **F**, Volcano plots (generated using the fold change and *q* values of DEGs) show differences between RA-CCP^{POS} B cells and RA-CCP^{NEG} B cells from the same donors. **G**, GO plot depicts the fold change in expression of genes related to immune responses that are highly expressed in RA-CCP^{POS} B cells compared to RA-CCP^{NEG} B cells from the same donors. See Figure 1 for other definitions. Color figure can be viewed in the online issue, which is available at <http://onlinelibrary.wiley.com/doi/10.1002/art.40772/abstract>.

they can promote B cell differentiation and Ig secretion (26). Similarly, the small macrophage-activating factor family of transcription factors (*MAFF* and *MAFG*), which have a direct impact on Ig secretion (27), were enriched in these RA-CCP^{POS} B cells (Figure 2E).

We also sought to determine whether there was a B cell-specific change in expression of genes known to be high-risk loci in RA, as has been documented through large-scale genetic studies (28). Of the known RA-specific loci, 9 genes were also identi-

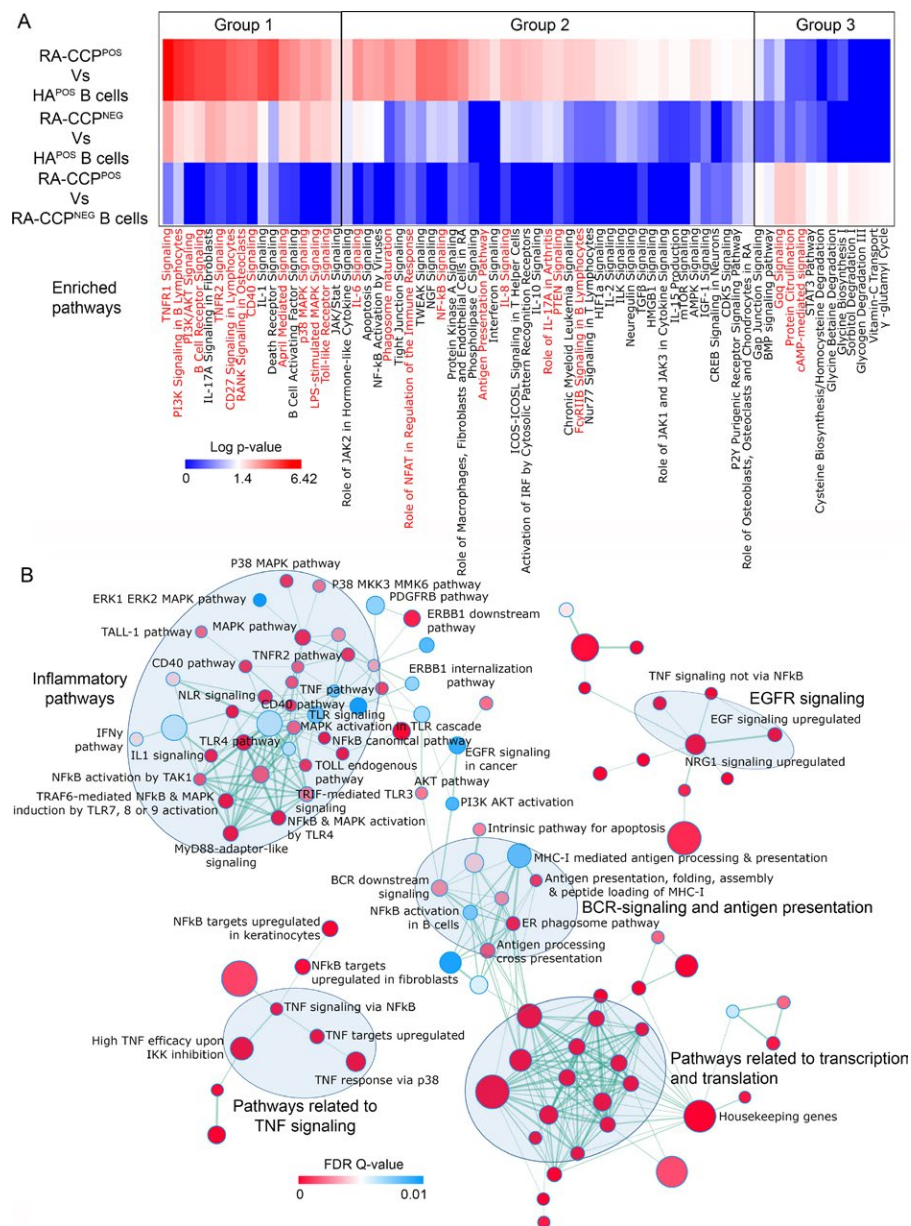


Figure 3. Enrichment maps of pathways enriched in RA-CCP^{POS} B cells compared to HA^{POS} B cells. **A**, Heatmaps were generated using log-transformed *P* values for differentially expressed gene pathways from Ingenuity Pathway Analysis, indicating enrichment of proinflammatory pathways in RA-CCP^{POS} B cells compared to HA^{POS} B cells, and up-regulation of protein citrullination in RA-CCP^{POS} B cells compared to RA-CCP^{NEG} B cells. Highlighted pathways are shown in red. **B**, The gene-set enrichment analysis–derived enriched C2 curated pathways in RA-CCP^{POS} B cells were plotted with the enrichment map application in Cytoscape, using a cutoff false discovery rate (FDR) *q* value of 0.01 and *P* value of 0.005. Nodes (red and blue circles) represent pathways, and the edges (green lines) represent overlapping genes among pathways. The size of nodes represents the number of genes enriched within the pathway, and the thickness of edges represents the number of overlapping genes. The color of nodes was adjusted to an FDR *q* value ranging from 0 to 0.01. Clusters of pathways are labeled as groups with a similar theme. All pathways represented are enriched in RA-CCP^{POS} B cell populations. TNFR1 = tumor necrosis factor receptor 1; PI3K = phosphatidylinositol 3-kinase; IL-17A = interleukin-17A; LPS = lipopolysaccharide; NGF = nerve growth factor; ICOS = inducible costimulator; IRF = interferon regulatory factor; FcγRIIb = Fcγ receptor type IIb; HIF1α = hypoxia-inducible factor 1α; ILK = integrin-linked kinase; TGFβ = transforming growth factor β; HMGB1 = high mobility group box chromosomal protein 1; mTOR = mechanistic target of rapamycin; AMPK = AMP-activated protein kinase; IGF-1 = insulin-like growth factor 1; BMP = bone morphogenetic protein; Gαq = G protein–coupled receptor; PDGFRB = platelet-derived growth factor β receptor; EGFR = endothelial growth factor receptor; TLR = Toll-like receptor; IFNγ = interferon-γ; TAK1 = TGFβ-activated kinase 1; NRG1 = neuregulin 1; TRAF6 = TNFR-associated factor 6; MyD88 = myeloid differentiation factor 88; MHC-I = class I major histocompatibility complex; BCR = B cell receptor; ER = endoplasmic reticulum (see Figure 1 for other definitions).

fied as DEGs (*SH2B3*, *CCR6*, *ILF3*, *TXNDC11*, *PTPRC*, *PRDM1*, *TNFAIP3*, *TRAF6*, and *LBH*) (see Supplementary Figures 3A–C, <http://onlinelibrary.wiley.com/doi/10.1002/art.40772/abstract>).

Comparisons between RA-CCP^{POS} and RA-CCP^{NEG}

B cells. The candidate DEGs that were up-regulated within the RA-CCP^{POS} B cell population, as compared to RA-CCP^{NEG} B cells within these same donors, included the pentraxin gene *PTX3* (Figures 2F and G), which recognizes pathogen-associated molecular patterns, and its binding partner in the complement cascade, *C1QB* (29,30), bone morphogenetic protein genes *BMP2* and *BMP5*, and PAD citrullinating enzyme genes *PADI2* and *PADI6* (31) (Figure 2F). In addition, several immune-related transcripts, such as inflammasome-associated protein gene *NLRP7* (32) and Fc receptor (FcR)-like protein gene *FCRL6* (33), were also up-regulated within RA-CCP^{POS} B cells (Figures 2F and G).

Cytokine and signaling pathways enriched in RA-CCP^{POS} B cells. The differentially expressed pathways were identified by matching the expression data set using Ingenuity Pathway Analysis (IPA), which filtered the pathways directly related to immune cells and their functions, and the results were visualized as a heatmap using the log *P* values (Figure 3A). In order to facilitate comparisons, we identified 3 groups of pathways that were enriched, in which group 1 comprised pathways in both the RA-CCP^{POS} and RA-CCP^{NEG} B cell populations compared to the HA^{POS} B cell population, group 2 comprised pathways enriched only in the RA-CCP^{POS} B cell population but not in the RA-CCP^{NEG} or HA^{POS} B cell populations, and group 3 comprised pathways enriched only in the RA-CCP^{POS} B cell population but not in the RA-CCP^{NEG} B cell population.

The pathways in group 1 were B cell activation pathways (B cell receptor signaling, phosphatidylinositol 3-kinase/AKT, and p38 MAPK), Toll-like receptor (TLR)-based activation pathways (TLR signaling and lipopolysaccharide-stimulated MAPK pathways), and TNF superfamily ligand-mediated signaling pathways (CD40, APRIL signaling) and their receptor signaling pathways (TNFR1, TNFR2, CD27, RANK, and CD40). The pathways in group 2 comprised inflammatory cytokine signaling (IL-6, IL-8, and IL-17A) and RA-specific signatures (role of macrophages, endothelial cells, and osteoclasts in RA), as well as pathways of B cell activation/homeostasis (PTEN, NF- κ B, and NFAT activation) and function (phagosome maturation, Fc γ R1b signaling, and antigen presentation). Finally, group 3 showed enrichment in pathways for protein citrullination, G protein-coupled receptor (G α q) signaling and cyclic AMP signaling (Figure 3A). Overall, whereas TNF signaling (group 1) has a global impact on all B cells from RA patients, these data suggest that RA-CCP^{POS} B cells, in comparison to RA-CCP^{NEG} B cells, demonstrate a potential role in protein citrullination and effector functionality.

Based on the substantially larger number of pathways and greater changes in expression identified by IPA in the RA-CCP^{POS} B cells in comparison to the HA^{POS} B cells (groups 1 and 2 combined), we performed gene-set enrichment analysis to compare

these 2 populations. We interrogated the changes in these populations against the Molecular Signatures Database (Hallmark and C2 curated gene sets). As shown in Figure 3B, 5 major clusters of pathways were significantly up-regulated (FDR *q* < 0.1) in the RA-CCP^{POS} B cells: 1) transcription and translation; 2) B cell receptor signaling; 3) EGF receptor (EGFR) signaling; 4) TNF signaling; and 5) inflammatory cytokines and chemokines.

Enrichment of *IL15RA* expression in RA-CCP^{POS} B cells from RA patients.

As outlined above, there was an abundance of cytokine and inflammation-related pathways found to be enriched in RA-CCP^{POS} B cells. We focused our attention on IL-15 signaling and performed enrichment analyses to compare our different B cell populations against known human IL-15-mediated signaling. RA-CCP^{POS} B cells showed a specific enrichment in IL-15-mediated signaling in comparison to either the HA^{POS} B cells or the RA-CCP^{NEG} B cells (Figures 4A and B).

We next examined the relative abundance of both *IL15* and its specific receptor, *IL15RA*. Indeed, *IL15RA* transcripts were up-regulated within RA-CCP^{POS} B cells relative to either RA-CCP^{NEG} or HA^{POS} B cells (Figure 4C). However, a significant difference in the expression of *IL15* was not observed (see Supplementary Figure 4, <http://onlinelibrary.wiley.com/doi/10.1002/art.40772/abstract>).

In order to validate the elevated expression of *IL15RA*, we utilized an independent cohort of CCP-seropositive RA patients and performed ex vivo surface staining on B cells by flow cytometry, using the same gating strategy as described earlier. Consistent with the RNA-seq results, there was a distinct subpopulation of RA-CCP^{POS} B cells that expressed IL-15R α in all of the patients tested, whereas this was clearly absent in either the RA-CCP^{NEG} or HA^{POS} B cell populations (Figure 4D and Supplementary Figure 5 [<http://onlinelibrary.wiley.com/doi/10.1002/art.40772/abstract>]). Interestingly, within the RA patients, 75–90% of IL-15R α -expressing IgG/IgA B cells were identified to be RA-CCP^{POS} B cells, thus indicating that IL-15R α expression was significantly enriched in this population (Figure 4E).

Since IL-15R α can also be converted to the soluble form by proteolytic cleavage via the TNF α -converting enzyme (TACE) (34), we next investigated the concentrations of soluble IL-15R α (sIL-15R α) in the RA patient cohort. Although elevated concentrations of sIL-15R α in the synovium are known to be associated with increased disease activity, there are no known reports that have documented elevated sIL-15R α concentrations in the serum of seropositive RA patients (35). To systematically validate a large number of candidate proteins within the RA patients' sera, including sIL-15R α , we took advantage of the aptamer-based SOMAscan assay, which can detect analytes at picomolar concentrations by utilizing very small volumes of biologic samples (36) (as depicted in Supplementary Figure 6, <http://onlinelibrary.wiley.com/doi/10.1002/art.40772/abstract>). In a cohort of CCP-seropositive RA patients (11 samples) compared to healthy donors (10 samples), we observed significantly higher

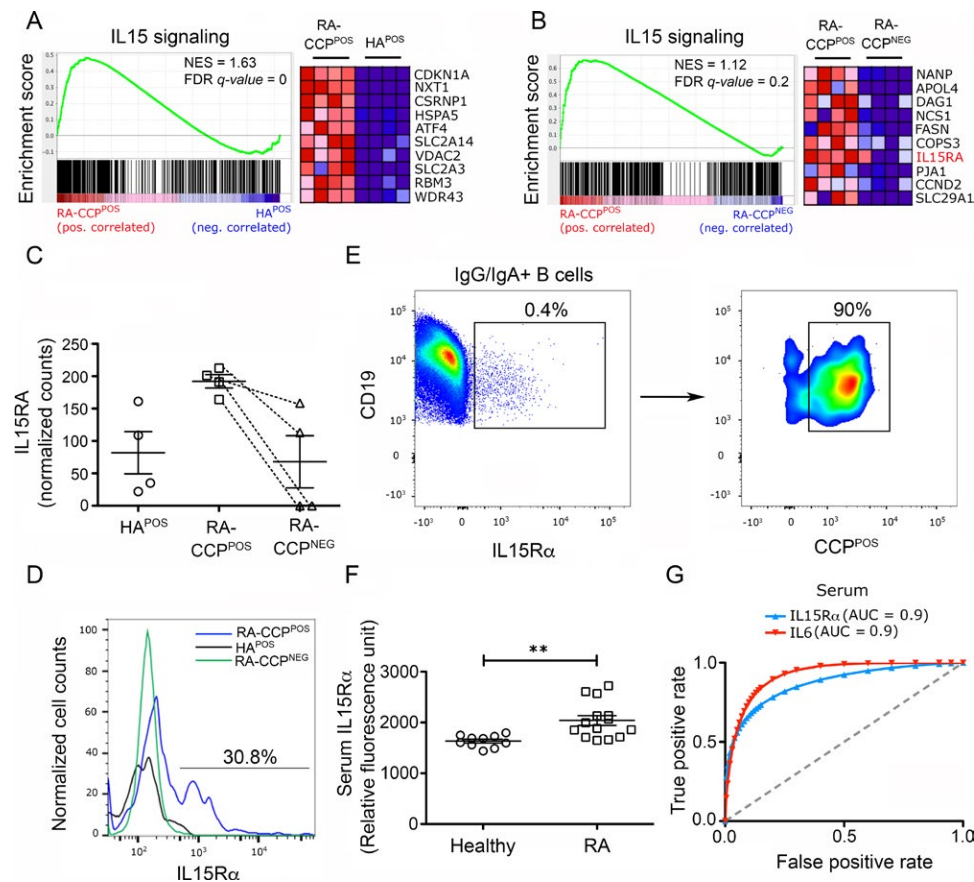


Figure 4. Interleukin-15 receptor α (IL-15R α) and IL-15 signaling are enriched in RA-CCP^{POS} B cells. **A** and **B**, Left, Gene-set enrichment analysis plots show positive correlations of IL-15 signaling in RA-CCP^{POS} B cells compared to HA^{POS} B cells (**A**) and RA-CCP^{POS} B cells compared to RA-CCP^{NEG} B cells (**B**). Right, Heatmaps show the top 10 genes enriched in the pathway using normalized transcript levels. **C**, Normalized transcript counts of *IL15RA* in RA-CCP^{POS}, RA-CCP^{NEG}, and HA^{POS} B cells are shown. Although nonparametric tests demonstrated significant differences between RA-CCP^{POS} B cells and the other 2 populations, since these would not account for multiple hypothesis testing, we have not shown these results. Horizontal lines with bars show the mean \pm SEM. **D**, Representative flow cytometric plots show IL-15R α expression on RA-CCP^{POS}, RA-CCP^{NEG}, and HA^{POS} B cells ($n = 4$ each). **E**, Expression of IL-15R α on RA-CCP^{POS} B cells is shown, gated on IL-15R α -positive IgG/IgA B cells ($n = 3$). Cells were sequentially gated as CD19+IgM/IgA-(IgG/IgA^{POS})IL-15R α ^{POS}CCP^{POS}. **F**, Concentrations of IL-15R α were determined in the serum of RA patients ($n = 11$) and healthy individuals ($n = 10$), as evaluated by SOMAScan. Horizontal lines with bars show the mean \pm SEM. ** = $P < 0.01$ by Mann-Whitney U test. **G**, Receiver operating characteristic (ROC) curves indicate the predictive value of IL-15R α and IL-6 serum levels for predicting the occurrence of RA. NES = normalized enrichment score; FDR = false discovery rate; AUC = area under the ROC curve (see Figure 1 for other definitions). Color figure can be viewed in the online issue, which is available at <http://onlinelibrary.wiley.com/doi/10.1002/art.40772/abstract>.

concentrations of both IL-6 and IL-8 in the RA patients, but no differences were seen in the concentrations of a large panel of other soluble analytes, including IL-1 β or IL-17 (see Supplementary Figure 7, <http://onlinelibrary.wiley.com/doi/10.1002/art.40772/abstract>). When we evaluated sIL-15R α , we observed significantly higher concentrations in the sera of RA patients in comparison to healthy controls (Figure 4F).

Finally, we also looked at the predictive value of serum sIL-15R α for the occurrence of CCP-seropositive RA, as determined by the SOMAScan assay, and found that sIL-15R α displayed both high sensitivity and high specificity for RA compared to healthy controls (Figure 4G). Using pROC, we confirmed the statistical power of sIL-15R α in this independent cohort of CCP-seropositive RA patients, which yielded a power estimate of 0.88.

EGFR pathways and molecular validation of AREG in

RA B cells. AREG is a member of the EGF family of ligands that signal through the EGFRs. It has been previously documented that TNF signaling in conjunction with IL-1 β signaling can lead to the up-regulation of AREG (34,37). Our data support a pivotal role of AREG in RA-CCP^{POS} B cells (Figure 5A), and also a role of its downstream target pathway, EGF-mediated signaling (Figure 5B).

In order to validate our findings, we used flow cytometry to directly interrogate the expression of AREG within individual B cells from an independent cohort of seropositive RA patients. As expected, we did not observe expression of AREG on RA-CCP^{POS} B cells ex vivo (see Supplementary Figure 8, <http://onlinelibrary.wiley.com/doi/10.1002/art.40772/abstract>), since AREG is secreted as a soluble protein upon cleavage by TACE (34).

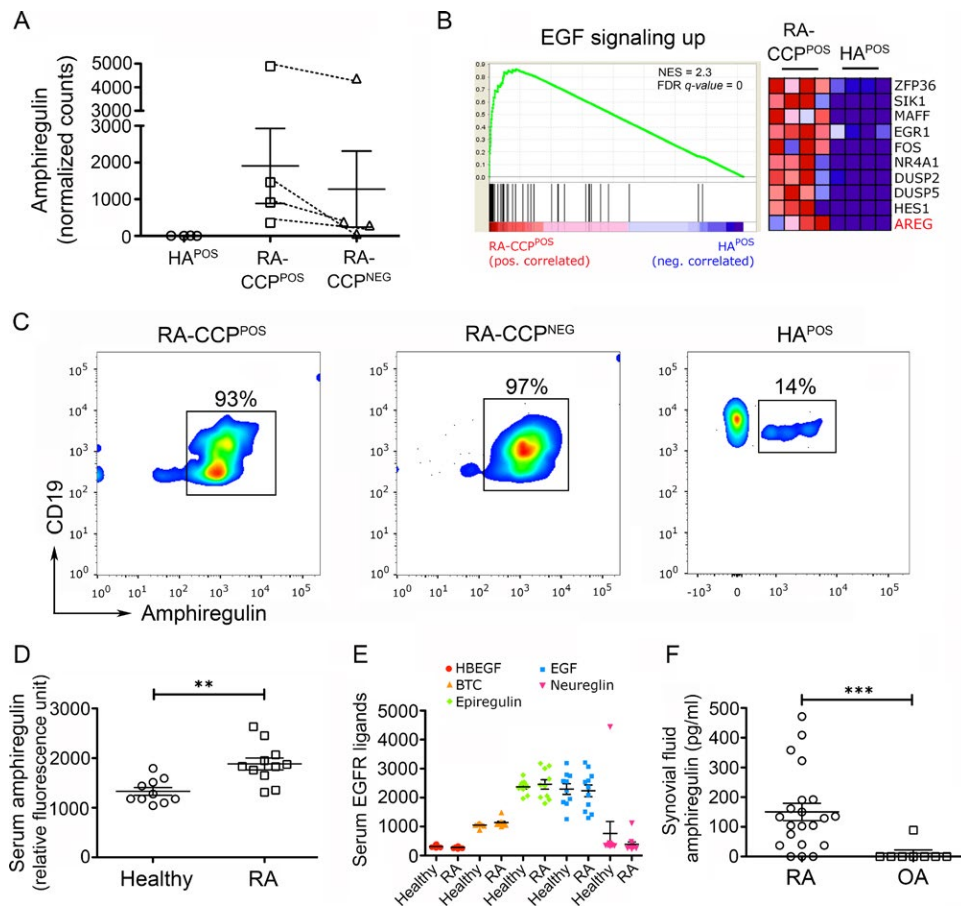


Figure 5. Amphiregulin (AREG) and associated pathways are enriched in RA-CCP^{POS} B cells. **A**, Normalized transcript counts of AREG in RA-CCP^{POS}, RA-CCP^{NEG}, and HA^{POS} B cells are shown. Although nonparametric tests demonstrated significant differences between RA-CCP^{POS} B cells and HA^{POS} B cells, since these would not account for multiple hypothesis testing, we have not shown these results. **B**, Left, Gene-set enrichment analysis plot shows the correlation of the epidermal growth factor (EGF) pathway in RA-CCP^{POS} versus HA^{POS} B cells. Right, Heatmap indicates normalized transcript levels of the top 10 genes in the pathway for each sample. **C**, AREG expression was evaluated by flow cytometry on RA-CCP^{POS}, RA-CCP^{NEG}, and HA^{POS} B cells after in vitro expansion ($n = 4$ each). **D**, Serum concentrations of AREG were determined in RA patients ($n = 11$) and healthy individuals ($n = 10$) by SOMAscan aptamer assay. The statistical power of this assay was estimated to be 0.98. **E**, Serum concentrations of all other EGF ligands in RA patients and healthy controls were identified by SOMAscan. **F**, Synovial fluid was assessed for AREG expression by enzyme-linked immunosorbent assay in patients with RA ($n = 21$) compared to patients with osteoarthritis (OA). In **A** and **D–F**, horizontal lines with bars show the mean \pm SEM. ** = $P < 0.01$; *** = $P < 0.001$, by Mann-Whitney U test. NES = normalized enrichment score; FDR = false discovery rate; HBEGF = heparin-binding EGF-like growth factor; BTC = betacellulin (see Figure 1 for other definitions). Color figure can be viewed in the online issue, which is available at <http://onlinelibrary.wiley.com/doi/10.1002/art.40772/abstract>.

In order to determine whether AREG expression can be induced in vitro in B cells, we sought to mimic the nature of help afforded by T helper cells in vivo in RA (38). Accordingly, populations of RA-CCP^{POS}, RA-CCP^{NEG}, and HA^{POS} B cells were sorted by flow cytometry and incubated with both soluble CD40L and IL-21 for 14 days. Under these conditions, both RA-CCP^{POS} and RA-CCP^{NEG} B cells showed induction of AREG in >80% of cells (Figure 5C), and this was consistent with our RNA-seq data on these populations (Figure 5A). A tendency toward higher expression of AREG was observed in RA-CCP^{POS} B cells compared to HA^{POS} B cells, but owing to the high variance in frequency of AREG-expressing HA^{POS} B cell populations, this change was not significant. Taken together, these findings suggest that under polarizing conditions, at least in vitro, B cells from RA patients act

as a source of AREG, a molecule with a known ability to have a global impact on multiple cell types.

Elevated expression of AREG in the serum and synovial fluid of RA patients. Among the different EGF ligands that are known to induce proliferation, growth, and differentiation by signaling through the EGFRs (39), AREG plays a unique role in its ability to induce both cell proliferation and cellular differentiation upon receptor binding (40). Although serum AREG levels in RA have been documented in other reports, these data are contradictory (41–43). We evaluated the concentrations of AREG and the other EGF ligands in the serum of CCP-seropositive RA patients, using the SOMAscan array as outlined above. In this cohort, we observed a significantly higher concentration of

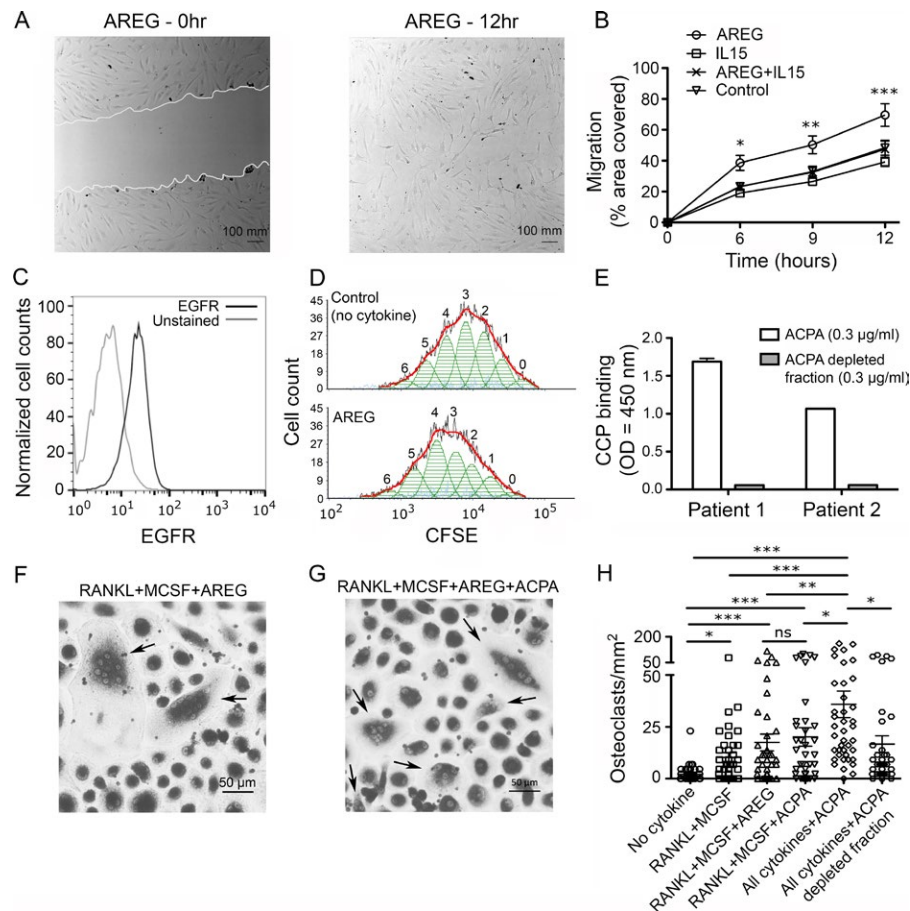


Figure 6. Amphiregulin (AREG) enhances migration and proliferation of fibroblast-like synoviocytes (FLS), and synergizes with anti-citrullinated protein antibodies (ACPAs) in mediating osteoclast differentiation. **A**, Representative scratch assay depicts cell migration at baseline and after 12 hours; experiments were performed twice, in triplicate, on FLS obtained from 1 rheumatoid arthritis (RA) patient. **B**, Migration of RA FLS, in response to AREG, interleukin-15 (IL-15), both AREG and IL-15, or a no cytokine control, is represented as the percentage of scratch area covered. Results are the mean \pm SEM. * = $P < 0.05$; ** = $P < 0.01$; *** = $P < 0.001$ versus control, by two-way analysis of variance. **C**, Expression of epidermal growth factor receptor (EGFR) on RA FLS is shown ($n = 3$ replicates). The light gray line represents unstained cells. **D**, Proliferation of FLS was measured using 5,6-carboxyfluorescein succinimidyl ester (CFSE) dilution ($n = 3$ replicates). **E**, Enrichment of ACPAs against cyclic citrullinated peptide (CCP) in the plasma of 2 RA patients was assessed by enzyme-linked immunosorbent assay ($n = 2$ replicates). **F** and **G**, Representative examples of differentiation of osteoclasts from blood monocytes under 2 different conditions are shown. **Arrows** indicate differentiated osteoclasts with ≥ 3 nuclei. **H**, The number of osteoclasts under different culture conditions is shown. ACPAs from 3 RA patients were used in conjunction with peripheral blood mononuclear cells from 3 healthy individuals ($n = 4$ replicates); 10 random images per well were obtained at an original magnification of $\times 20$. * = $P < 0.05$; ** = $P < 0.01$; *** = $P < 0.001$, by Kruskal-Wallis test with Dunn's test for multiple comparisons. Horizontal lines with bars show the mean \pm SEM in **B** and **H**, and mean \pm SD in **E**. MCSF = macrophage colony-stimulating factor; ns = not significant. Color figure can be viewed in the online issue, which is available at <http://onlinelibrary.wiley.com/doi/10.1002/art.40772/abstract>.

AREG in the serum of RA patients (Figure 5D), but no differences were seen in the concentrations of any of the other EGF ligands investigated, such as heparin-binding EGF-like growth factor, betacellulin, epiregulin, EGF, and neuregulin (Figure 5E).

In addition, we observed a high sensitivity and high specificity of serum AREG in predicting the occurrence of RA (see Supplementary Figure 9, <http://onlinelibrary.wiley.com/doi/10.1002/art.40772/abstract>). The estimated statistical power of serum AREG concentrations for prediction of RA in our cohort was 0.98.

Since RA is a disease with localized inflammation, we further evaluated the abundance of AREG in the synovial fluid from

CCP-seropositive RA patients (21 samples) and compared it with synovial fluid samples from patients with noninflammatory osteoarthritis (OA) (8 samples). Our ELISA results showed that the levels of AREG were significantly higher in RA synovial fluid compared to OA synovial fluid (only 1 OA synovial fluid sample tested positive for AREG) (Figure 5F).

Promotion of migration and proliferation of FLS in vitro by AREG. One of the hallmarks of RA pathogenesis is the activation of FLS, which is characterized by a tumor-like aggressive phenotype within the joints (44). We tested the ability of AREG to increase the invasiveness of human RA FLS,

and observed that AREG promoted the increased migration of FLS, in comparison to controls, in wound-healing assays (Figures 6A and B). We confirmed the expression of EGFR on RA FLS, suggesting that the increased invasiveness was likely attributable to increased AREG-induced EGFR signaling (Figure 6C).

We also observed that RA FLS proliferated more intensely in the presence of AREG in comparison to control FLS (Figure 6D). Taken together, our results thus indicate that high levels of AREG in the peripheral blood and synovial fluid of RA patients could be responsible for the aggressive phenotype of FLS in these patients.

Functional synergy between AREG and ACPAs in mediating osteoclastogenesis. The role of AREG in promoting osteolytic activity has been detailed as one of the mediators of bone metastases in breast cancers (45). Independently, the role of ACPAs in enabling osteoclast differentiation has been described in RA (4). We thus interrogated the functional synergy between these molecules in mediating osteoclastogenesis. First, we purified ACPAs by binding to a CCP-functionalized column (Figure 6E). Next, we evaluated the ability of each of these molecules, either by themselves or in combination, to promote the differentiation of multinucleated tartrate-resistant acid phosphatase-positive osteoclasts from monocyte precursors. Although AREG by itself did not significantly increase the differentiation of osteoclasts, the number of osteoclasts was observed to be higher in cocultures with AREG and ACPAs as compared to all other conditions tested (Figures 6F–H). Our findings thus suggest that AREG can synergize with ACPAs in the differentiation of osteoclasts from blood monocytes.

DISCUSSION

The role of RA-CCP^{POS} B cells as a source of autoantibodies contributing to disease pathology in RA has been extensively studied, but the functional programs that help define the biology of the cell have remained elusive. One of the challenges we encountered was the robust and reliable identification of RA-CCP^{POS} B cells, which accounts for <0.1% of total peripheral B cells in RA patients (14). We successfully designed a sensitive flow cytometric sorting method using peptide–streptavidin conjugates, and sorted both the IgG^{POS} and IgA^{POS} CCP^{POS} B cells, owing to the fact that the antibody response against citrullinated proteins in RA comprises both IgG- and IgA-type immunoglobulins (46).

Based on the RNA-seq data, we confirmed that the expression of the IL-15R α protein on the cell surface was enriched in the RA-CCP^{POS} B cell population, and also confirmed that increased levels of sIL-15R α could be detected within the blood of an independent cohort of CCP-seropositive RA patients. IL-

15-mediated signaling has been targeted in phase I and phase II clinical trials using HuMax-IL15 (see Supplementary Table 2, <http://onlinelibrary.wiley.com/doi/10.1002/art.40772/abstract>), a human monoclonal antibody that inhibits the bioactivity of IL-15 and that has produced modest improvements in disease activity (47). Synthetic disease-modifying antirheumatic drugs, including tofacitinib (a JAK inhibitor), can inhibit pathways that are also downstream of IL-15R α -derived signaling (48). Our data suggest that the targeting of IL-15R α might provide therapeutic benefit in RA, either by directly targeting the RA-CCP^{POS} B cells or by the elimination of sIL-15R α in the blood of RA patients. In this regard, it is worth emphasizing that sIL-15R α is known to increase the potency of IL-15 function by 100-fold when complexed together, and enables signaling in cells that might otherwise lack IL-15R α (49). As suggested previously, the enrichment of IL-15R α expression within the RA-CCP^{POS} B cells might be indicative of an altered differentiation state (50).

Our data are the first to reveal the expression of the EGFR ligand AREG on autoreactive B cells, which was also the most differentially expressed gene in RA-CCP^{POS} B cells as compared to HA^{POS} B cells. We confirmed the surface expression of AREG on B cells under inflammatory conditions, identified AREG as a candidate biomarker in CCP-seropositive RA, and evaluated the functional impact of AREG on the cellular effectors of RA. AREG is expressed as a membrane-bound molecule, which is activated upon proteolytic cleavage by TACE (34), thereby acting in an auto-crine or paracrine manner and influencing cell survival, proliferation, and motility (51).

Previously reported studies are contradictory with regard to AREG concentrations in the blood of RA patients, with evidence of both significantly increased concentrations and no significant differences in comparison to healthy donors (41–43). One confounding factor in these reports is CCP seropositivity. Consistent with our studies with RA-CCP^{POS} B cells, our results herein demonstrate significant increases in the concentration of AREG in the blood of CCP-seropositive RA patients in comparison to healthy donors. In parallel, immunohistochemistry has confirmed the expression of both AREG and EGFR within the synovial tissue of RA patients (34,42). Investigations using a mouse model of inflammation in RA, in which mice harbored the transgenic IL-6 signal transducer gene, have shown the importance of EGFs, including AREG, in the pathogenesis of arthritis, since targeting AREG either by neutralizing antibodies or by short-hairpin RNA ameliorated the disease severity (43).

The induction of AREG expression is governed by the cytokines transforming growth factor β (TGF β), TNF, and IL-1 β (34,37), which are known to be abundant in RA synovial fluid and plasma (52) (results for TGF β are shown in Supplementary Figure 10, <http://onlinelibrary.wiley.com/doi/10.1002/art.40772/abstract>). Our data illustrate that AREG can directly promote the proliferation and invasiveness of FLS. As outlined by elegant studies in breast cancer metastasis models, AREG is

also known to increase the differentiation and activity of osteoclasts from PBMCs in the presence of RANKL and macrophage colony-stimulating factor (45), both of which are abundantly available in the synovial compartment of RA patients. Our in vitro data further highlight the ability of AREG to act in concert with ACPAs to enhance the differentiation of osteoclasts from blood monocytes. Since our RNA-seq data outlined a role for both *IL6ST* and IL-6 signaling in RA-CCP^{POS} B cells, this suggests that IL-6 signaling might facilitate AREG up-regulation. Overall, our results indicate that under proinflammatory conditions, all B cells in RA may contribute to the production of AREG irrespective of antigen specificity, which may potentially affect other cells in the joints.

Through this study, we are reporting for the first time a comprehensive transcriptome profile of RA-CCP^{POS} B cells in RA. To the best of our knowledge, this is also the first study to conduct whole transcriptome profiling of antigen-specific B cells in any human autoimmune disorder. Our results portray B cells not merely as autoantibody producers, but also as a source of diverse molecules that can influence proliferation, differentiation, and activation of other pathogenic cell types. We anticipate that these data will serve as a foundational data set for investigating multiple hypotheses on the roles of B cells in RA and other autoimmune disorders, and will enable drug discovery and validation based on the biology of RA-CCP^{POS} B cells in RA.

We also recognize that although our report represents an important first step, further studies are required to gain a much deeper understanding of autoreactive B cells in autoimmune biology. Comprehensive studies on the relationships between sIL-15R α and AREG within the synovial compartment, and all of the different cell types that can secrete these molecules and how they influence the expression and secretion of each other and other signaling cascades, need to be performed. Although direct profiling of synovial B cells can reflect their contribution to RA pathophysiology, obtaining these cells is challenging from a clinical perspective. Arthroscopy is considered an invasive procedure and hence not routinely performed in clinical practice. Similarly, although synovial tissue can be accessed from patients undergoing joint replacement, these patients have end-stage disease not reflective of therapeutically relevant disease. Moreover, although single-cell RNA-seq (scRNA-seq) is better suited for studying moderately or highly expressed transcripts, it would be interesting to perform scRNA-seq to document the heterogeneity in autoimmune B cells, to complement our existing results, especially with synovial B cells.

ACKNOWLEDGMENTS

We would like to acknowledge the University of Houston Seq-n-edit core for the RNA-seq data analyses, Intel for the loan of the computing cluster, and the University of Houston Center for Advanced Computing and Data Systems for providing the high-performance computing facilities.

AUTHOR CONTRIBUTIONS

All authors were involved in drafting the article or revising it critically for important intellectual content, and all authors approved the final version to be published. Dr. Varadarajan had full access to all of the data in the study and takes responsibility for the integrity of the data and the accuracy of the data analysis.

Study conception and design. Mahendra, Varadarajan.

Acquisition of data. Mahendra, Abnoui, Soomro, Wanzeck, Bridges, Aggarwal, Agarwal, Mohan, Varadarajan.

Analysis and interpretation of data. Mahendra, Yang, Adolacion, Park, Roszik, Coarfa, Romain, Qiu, Varadarajan.

REFERENCES

1. Van der Linden MP, van der Woude D, Ioan-Facsinay A, Levarht EW, Stoecken-Rijsbergen G, Huizinga TW, et al. Value of anti-modified citrullinated vimentin and third-generation anti-cyclic citrullinated peptide compared with second-generation anti-cyclic citrullinated peptide and rheumatoid factor in predicting disease outcome in undifferentiated arthritis and rheumatoid arthritis. *Arthritis Rheum* 2009;60:2232–41.
2. Wagner CA, Sokolove J, Lahey LJ, Bengtsson C, Saevarsdottir S, Alfredsson L, et al. Identification of anticitrullinated protein antibody reactivities in a subset of anti-CCP-negative rheumatoid arthritis: association with cigarette smoking and HLA-DRB1 ‘shared epitope’ alleles. *Ann Rheum Dis* 2015;74:579–86.
3. Boross P, Verbeek JS. The complex role of Fc γ receptors in the pathology of arthritis. *Springer Semin Immunopathol* 2006;28:339–50.
4. Harre U, Georgess D, Bang H, Bozec A, Axmann R, Ossipova E, et al. Induction of osteoclastogenesis and bone loss by human autoantibodies against citrullinated vimentin. *J Clin Invest* 2012;122:1791–802.
5. Dorner T, Radbruch A, Burmester GR. B-cell-directed therapies for autoimmune disease. *Nat Rev Rheumatol* 2009;5:433–41.
6. Lal P, Su Z, Holweg CT, Silverman GJ, Schwartzman S, Kelman A, et al. Inflammation and autoantibody markers identify rheumatoid arthritis patients with enhanced clinical benefit following rituximab treatment. *Arthritis Rheum* 2011;63:3681–91.
7. Toubi E, Kessel A, Slobodin G, Boulman N, Pavlotzky E, Zisman D, et al. Changes in macrophage function after rituximab treatment in patients with rheumatoid arthritis. *Ann Rheum Dis* 2007;66:818–20.
8. Takemura S, Klimiuk PA, Braun A, Goronzy JJ, Weyand CM. T cell activation in rheumatoid synovium is B cell dependent. *J Immunol* 2001;167:4710–8.
9. Barr TA, Shen P, Brown S, Lampropoulou V, Roch T, Lawrie S, et al. B cell depletion therapy ameliorates autoimmune disease through ablation of IL-6-producing B cells. *J Exp Med* 2012;209:1001–10.
10. McInnes IB, Schett G. Cytokines in the pathogenesis of rheumatoid arthritis. *Nat Rev Immunol* 2007;7:429–42.
11. Kalliolias GD, Ivaschkiv LB. TNF biology, pathogenic mechanisms and emerging therapeutic strategies. *Nat Rev Rheumatol* 2016;12:49–62.
12. Takemura S, Braun A, Crowson C, Kurtin PJ, Cofield RH, O’Fallon WM, et al. Lymphoid neogenesis in rheumatoid synovitis. *J Immunol* 2001;167:1072–80.
13. Meedhu N, Zhang H, Owen T, Sun W, Wang V, Cistrone C, et al. Production of RANKL by memory B cells: a link between B cells and bone erosion in rheumatoid arthritis. *Arthritis Rheumatol* 2016;68:805–16.
14. Kerkman PF, Fabre E, van der voort EI, Zaldumbide A, Rombouts Y, Rispen S, et al. Identification and characterisation of citrullinated antigen-specific B cells in peripheral blood of patients with rheumatoid arthritis. *Ann Rheum Dis* 2016;75:1170–6.
15. Arnett FC, Edworthy SM, Bloch DA, McShane DJ, Fries JF, Cooper NS, et al. The American Rheumatism Association 1987 revised

- criteria for the classification of rheumatoid arthritis. *Arthritis Rheum* 1988;31:315–24.
16. Van der Maaten L, Hinton G. Visualizing data using t-SNE. *J Mach Learn Res* 2008;9:2579–605.
 17. Vieth B, Ziegenhain C, Parekh S, Enard W, Hellmann I. PowsimR: power analysis for bulk and single cell RNA-seq experiments. *Bioinformatics* 2017;33:3486–8.
 18. Santiago-Raber ML, Lawson BR, Dummer W, Barnhouse M, Koundouris S, Wilson CB, et al. Role of cyclin kinase inhibitor p21 in systemic autoimmunity. *J Immunol* 2001;167:4067–74.
 19. Chang M, Jin W, Chang JH, Xiao Y, Brittain GC, Yu J, et al. The ubiquitin ligase Peli1 negatively regulates T cell activation and prevents autoimmunity. *Nat Immunol* 2011;12:1002–9.
 20. Hamel KM, Cao Y, Olalekan SA, Finnegan A. B cell-specific expression of inducible costimulator ligand is necessary for the induction of arthritis in mice. *Arthritis Rheumatol* 2014;66:60–7.
 21. Werner M, Hobeika E, Jumaa H. Role of PI3K in the generation and survival of B cells. *Immunol Rev* 2010;237:55–71.
 22. Thalhamer T, McGrath MA, Harnett MM. MAPKs and their relevance to arthritis and inflammation. *Rheumatology (Oxford)* 2008;47:409–14.
 23. Kurko J, Besenyi T, Laki J, Glant TT, Mikecz K, Szekanecz Z. Genetics of rheumatoid arthritis: a comprehensive review. *Clin Rev Allergy Immunol* 2013;45:170–9.
 24. Nagafuchi Y, Shoda H, Sumitomo S, Nakachi S, Kato R, Tsuchida Y, et al. Immunophenotyping of rheumatoid arthritis reveals a linkage between HLA-DRB1 genotype, CXCR4 expression on memory CD4(+) T cells, and disease activity. *Sci Rep* 2016;6:29338.
 25. Lin Y, Wong K, Calame K. Repression of c-myc transcription by Blimp-1, an inducer of terminal B cell differentiation. *Science* 1997;276:596–9.
 26. Nutt SL, Fairfax KA, Kallies A. BLIMP1 guides the fate of effector B and T cells. *Nat Rev Immunol* 2007;7:923–7.
 27. Muto A, Hoshino H, Madisen L, Yanai N, Obinata M, Karasuyama H, et al. Identification of Bach2 as a B-cell-specific partner for small MAF proteins that negatively regulate the immunoglobulin heavy chain gene 3' enhancer. *EMBO J* 1998;17:5734–43.
 28. Eyre S, Bowes J, Diogo D, Lee A, Barton A, Martin P, et al. High-density genetic mapping identifies new susceptibility loci for rheumatoid arthritis. *Nat Genet* 2012;44:1336–40.
 29. Moalli F, Jaillon S, Inforzato A, Sironi M, Bottazzi B, Mantovani A, et al. Pathogen recognition by the long pentraxin PTX3. *J Biomed Biotechnol* 2011;2011:830421.
 30. Roumenina LT, Ruseva MM, Zlatarova A, Ghai R, Kolev M, Olova N, et al. Interaction of C1q with IgG1, C-reactive protein and pentraxin 3: mutational studies using recombinant globular head modules of human C1q A, B, and C chains. *Biochemistry* 2006;45:4093–104.
 31. Wang S, Wang Y. Peptidylarginine deiminases in citrullination, gene regulation, health and pathogenesis. *Biochim Biophys Acta* 2013;1829:1126–35.
 32. Khare S, Luc N, Dorfleutner A, Stehlik C. Inflammasomes and their activation. *Crit Rev Immunol* 2010;30:463–87.
 33. Schreeder DM, Cannon JP, Wu J, Li R, Shakhmatov MA, Davis RS. Cutting edge: FcR-like 6 is an MHC class II receptor. *J Immunol* 2010;185:23–7.
 34. Liu FL, Wu CC, Chang DM. TACE-dependent amphiregulin release is induced by IL-1 β and promotes cell invasion in fibroblast-like synoviocytes in rheumatoid arthritis. *Rheumatology (Oxford)* 2014;53:260–9.
 35. Santos Savio A, Machado Diaz AC, Chico Capote A, Miranda Navarro J, Rodríguez Alvarez Y, Bringas Pérez R, et al. Differential expression of pro-inflammatory cytokines IL-15R α , IL-15, IL-6 and TNF α in synovial fluid from rheumatoid arthritis patients. *BMC Musculoskelet Disord* 2015;16:51.
 36. Albaba D, Soomro S, Mohan C. Aptamer-based screens of human body fluids for biomarkers. *Microarrays (Basel)* 2015;4:424–31.
 37. Woodworth CD, McMullin E, Iglesias M, Plowman GD. Interleukin 1 α and tumor necrosis factor α stimulate autocrine amphiregulin expression and proliferation of human papillomavirus-immortalized and carcinoma-derived cervical epithelial cells. *Proc Natl Acad Sci U S A* 1995;92:2840–4.
 38. Rao DA, Gurish MF, Marshall JL, Slowikowski K, Fonseka CY, Liu Y, et al. Pathologically expanded peripheral T helper cell subset drives B cells in rheumatoid arthritis. *Nature* 2017;542:110–4.
 39. Wieduwilt MJ, Moasser MM. The epidermal growth factor receptor family: biology driving targeted therapeutics. *Cell Mol Life Sci* 2008;65:1566–84.
 40. Zaiss DM, Gause WC, Osborne LC, Artis D. Emerging functions of amphiregulin in orchestrating immunity, inflammation, and tissue repair. *Immunity* 2015;42:216–26.
 41. Yamane S, Ishida S, Hanamoto Y, Kumagai K, Masuda R, Tanaka K, et al. Proinflammatory role of amphiregulin, an epidermal growth factor family member whose expression is augmented in rheumatoid arthritis patients. *J Inflamm (Lond)* 2008;5:5.
 42. Swanson CD, Akama-Garren EH, Stein EA, Petralia JD, Ruiz PJ, Edalati A, et al. Inhibition of epidermal growth factor receptor tyrosine kinase ameliorates collagen-induced arthritis. *J Immunol* 2012;188:3513–21.
 43. Harada M, Kamimura D, Arima Y, Kohsaka H, Nakatsuji Y, Nishida M, et al. Temporal expression of growth factors triggered by epiregulin regulates inflammation development. *J Immunol* 2015;194:1039–46.
 44. Bartok B, Firestein GS. Fibroblast-like synoviocytes: key effector cells in rheumatoid arthritis. *Immunol Rev* 2010;233:233–55.
 45. Bolin C, Tawara K, Sutherland C, Redshaw J, Aranda P, Moselhy J, et al. Oncostatin M promotes mammary tumor metastasis to bone and osteolytic bone degradation. *Genes Cancer* 2012;3:117–30.
 46. Kokkonen H, Mullazehi M, Berglin E, Hallmans G, Wadell G, Rönnelid J, et al. Antibodies of IgG, IgA and IgM isotypes against cyclic citrullinated peptide precede the development of rheumatoid arthritis. *Arthritis Res Ther* 2011;13:R13.
 47. Baslund B, Tvede N, Danneskiold-Samsøe B, Larsson P, Panayi G, Petersen J, et al. Targeting interleukin-15 in patients with rheumatoid arthritis: a proof-of-concept study. *Arthritis Rheum* 2005;52:2686–92.
 48. Waldmann TA. The biology of IL-15: implications for cancer therapy and the treatment of autoimmune disorders. *J Invest Dermatol Symp Proc* 2013;16:S28–30.
 49. Machado Diaz AC, Chico Capote A, Arrieta Aguero CA, Rodríguez Alvarez Y, García Del Barco Herrera D, Estévez Del Toro M, et al. Proinflammatory soluble interleukin-15 receptor α is increased in rheumatoid arthritis. *Arthritis* 2012;2012:943156.
 50. Tarte K, Zhan F, De Vos J, Klein B, Shaughnessy J Jr. Gene expression profiling of plasma cells and plasmablasts: toward a better understanding of the late stages of B-cell differentiation. *Blood* 2003;102:592–600.
 51. Berasain C, Avila MA. Amphiregulin. *Semin Cell Dev Biol* 2014;28:31–41.
 52. Tetta C, Camussi G, Modena V, Di Vittorio C, Baglioni C. Tumour necrosis factor in serum and synovial fluid of patients with active and severe rheumatoid arthritis. *Ann Rheum Dis* 1990;49:665–7.